

Three-dimensional graphene encapsulated Ag-ZnFe₂O₄ flower-like nanocomposites with enhanced photocatalytic degradation of enrofloxacin

Kangwang Wang^a, Sheng Zhan^b, Danyang Zhang^c, Hui Sun^b, Xiaodong Jin^a, Juan Wang^{c,d,*}

^a School of Chemical and Biological Engineering, Lanzhou Jiaotong University, Lanzhou, 730070, P.R. China.

^b School of Materials Science and Engineering, Shaanxi Normal University, Xi'an, 710119, P.R. China.

^c School of Chemistry and Chemical Engineering, Shaanxi Normal University, Xi'an, 710062, P. R. China.

^d School of medicine, Shaanxi Institute of International Trade & Commerce, Xi'an, 712046, P. R. China.

Experimental Section

Synthesis of materials

FeCl₃·6H₂O, and urea were purchased from Fu Chen Chemical Reagent Co., Ltd. (Tianjin, China). ZnCl₂ was purchased from Acros Organics with a purity of over 99.9%. Silver nitrate (AgNO₃, 99.8%) was supplied by Aladdin Reagent Co., Ltd. (Shanghai, China). Ethylene glycol (EG) were purchased from Shanghai Chemical Reagent Factory. Graphene was purchased from Sinopharm Chemical Reagent Beijing Co., Ltd. All of the reagents used in our experiments are analytical purity and used without further purification. Enrofloxacin (ENR) was selected from Aladdin industrial corporation, Sinopharm. Milli-Q water (a minimum resistivity of 18.25 MΩ cm) was used as the solvent for all the solutions or dispersions.

Materials characterization

Scanning electron microscopic (SEM) images of the samples were obtained on a JEOL-JEM-2010 (JEOL, Japan) operating at 200 kV, which was equipped with an energy-dispersive X-ray spectroscope (EDS) operated at an acceleration voltage of 12 kV. Transmission electron microscopic (TEM) imaging was taken with a FEI Titan Themis 200 TEM at an acceleration voltage of 200 kV. The X-ray powder diffraction (XRD) was used with Cu-Kα radiation ($\lambda = 1.506 \text{ \AA}$) and the range of 2θ is from 10° to ~ 90° (D/max-2500, Rigaku, Japan). X-ray photoelectron spectroscopy (XPS) was carried out by Thermo Fisher scientific (ESCLAB 250 Xi England). The Brunauer-Emmett-Teller (BET) specific surface areas and porosity of the Ag-ZnFe₂O₄-rGO were determined using micromeritics (ASAP 2460 U.S.A.) surface area and porosity analyzer. The magnetism of the Ag-ZnFe₂O₄-rGO was obtained by vibrating sample magnetometer (MPMS (SQUID) XL, Quantum Design, America) analysis. The optical absorption of Ag-ZnFe₂O₄-rGO was examined by a spectrophotometer (Cary 5000, Varian) with an integrating sphere attachment in the range of 200 nm ~ 800 nm to record its diffuse reflectance spectrum (DRS), in which a baseline was recorded using BaSO₄. The Fourier-transform infrared (FT-IR) spectra were performed using Avatar 360 (Nicolet Instrument Corporation, US) in a wavenumber from 4000 cm⁻¹ ~ 400 cm⁻¹ to characterize the surface

* Corresponding author.

E-mail addresses: wangvipjuan@163.com (J. Wang).

functionalized groups of the samples. Photoluminescence (PL) spectra was recorded on a F-4600 fluorescence spectrophotometer with an excitation wavelength of 361 nm.

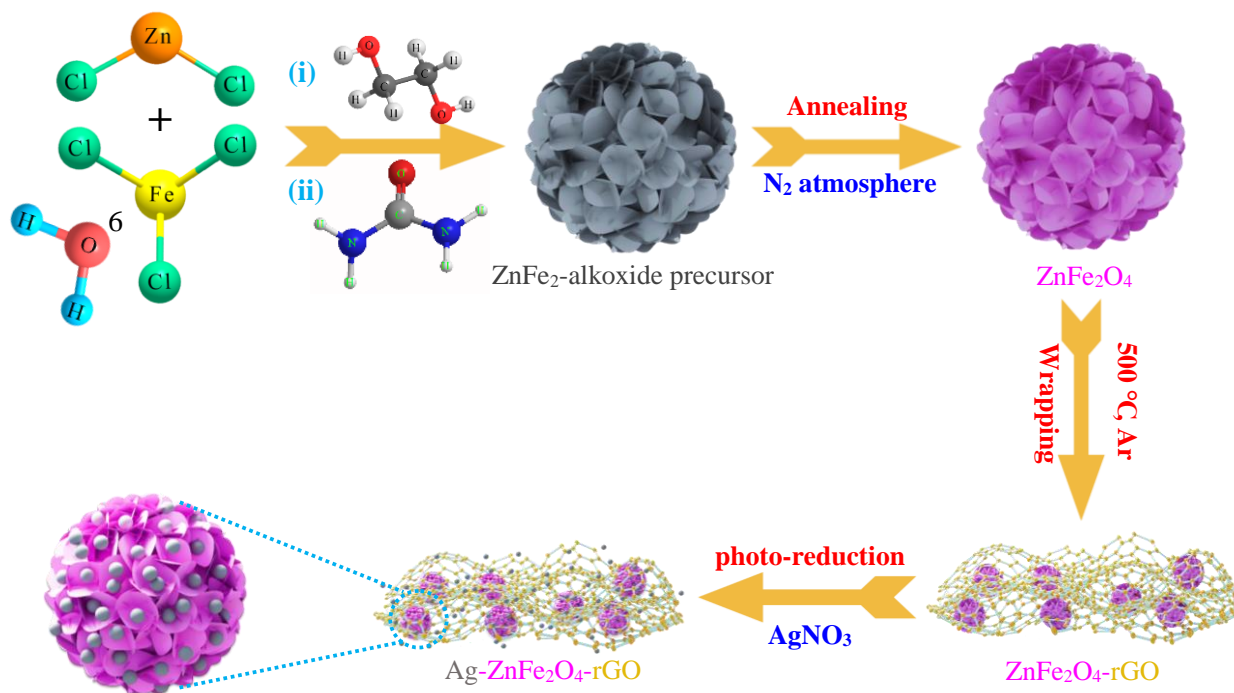


Fig. S1 Schematic illustration of the preparation process for the Ag-ZnFe₂O₄-rGO nanocomposites.

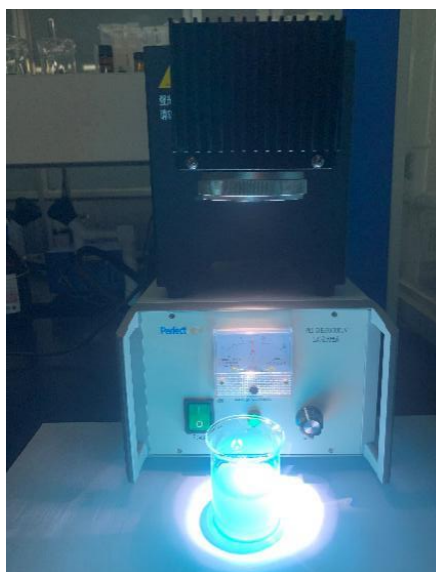


Fig. S2 Schematic diagram of the photocatalytic degradation of ENR experiment process.

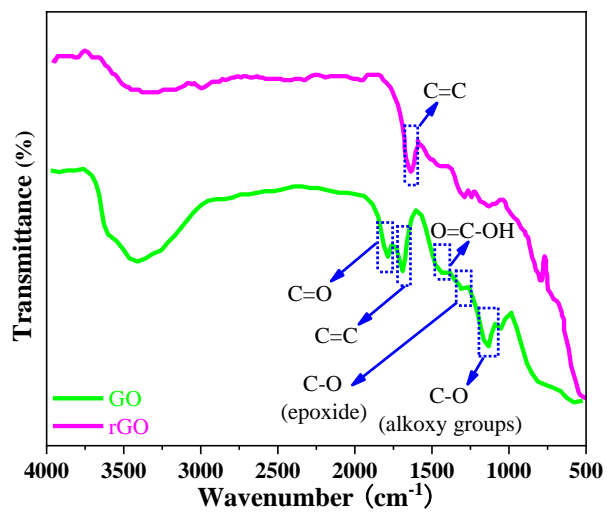


Fig. S3 FT-IR spectra of the GO and rGO samples.

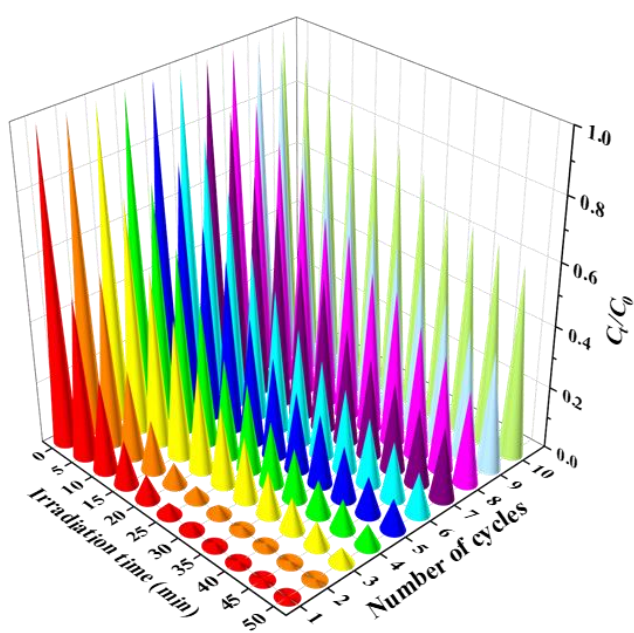


Fig. S4 10 consecutive cycling photodegradation activities of ENR ($10 \text{ mg}\cdot\text{L}^{-1}$) aqueous solution over the $\text{Ag-ZnFe}_2\text{O}_4\text{-rGO}$ photocatalysts under visible-light ($\lambda = 465 \text{ nm}$) irradiation, respectively.

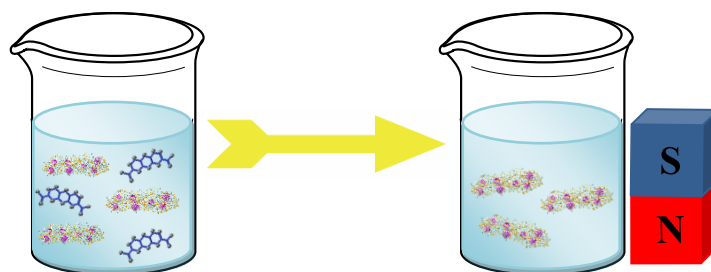


Fig. S5 Schematic diagram of photocatalytic degradation recycling.

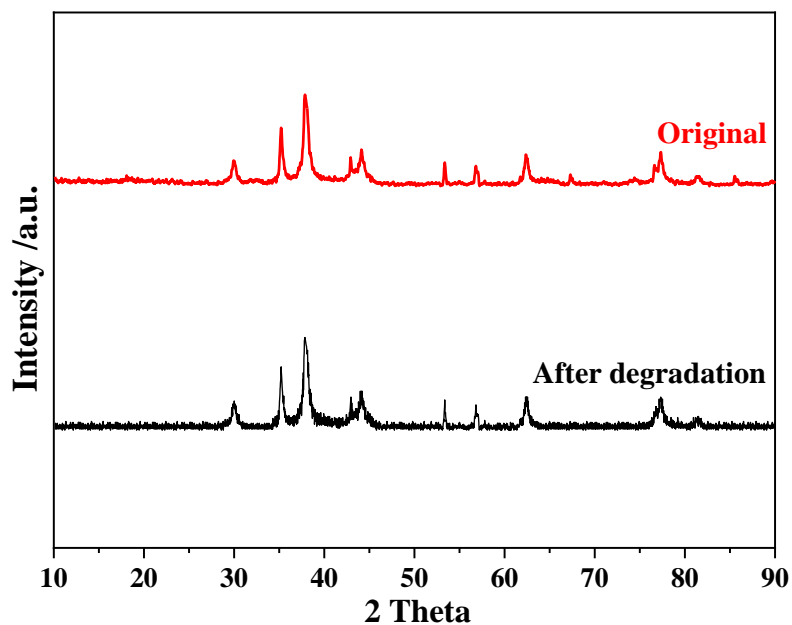


Fig. S6 XRD pattern of original Ag-ZnFe₂O₄-rGO and after degradation (10 cycles).

Table. S1 Comparison study of a magnetic photocatalyst.

Materials	Model pollutants	Source of light	Photocatalytic degradation	
			k_{obs}	Ref
Graphene-WO ₃	ENR	a solar simulator (100 mW/cm ²)	0.072 min ⁻¹	1
g-C ₃ N ₄ /Bi ₂ WO ₆ /AgI	ENR	300 W Xenon lamp ($\lambda = 420$ nm)	0.0223 min ⁻¹	2
g-C ₃ N ₄ -Mg	ENR	300 W Xenon lamp ($\lambda > 420$ nm)	0.014 min ⁻¹	3
GaOOH/ZnBiNbO ₅	ENR	a mercury lamp (500 W)	0.02064 min ⁻¹	4

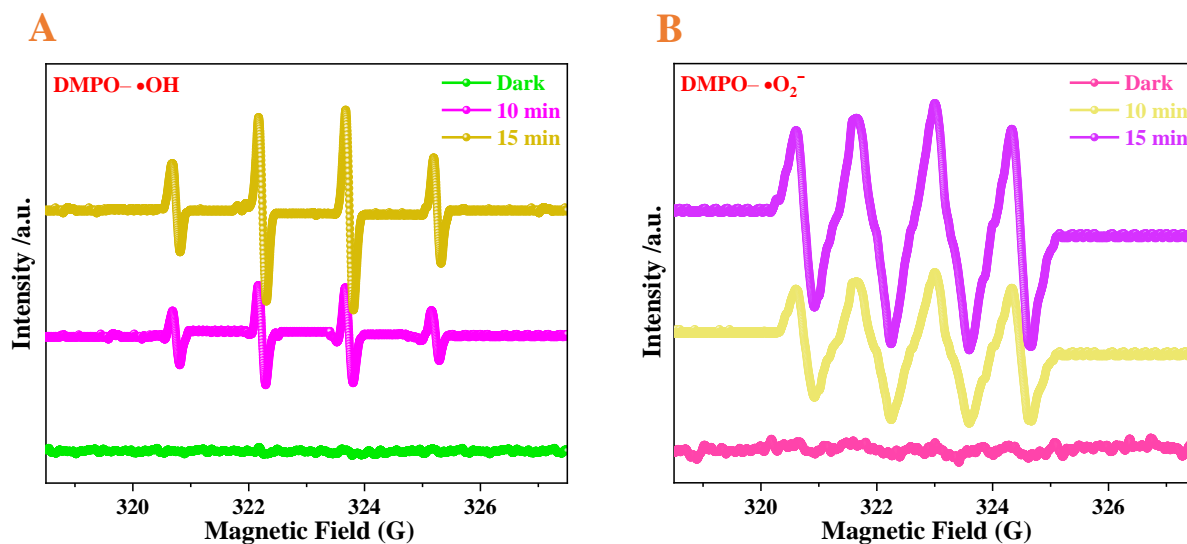
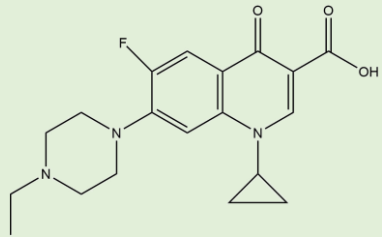
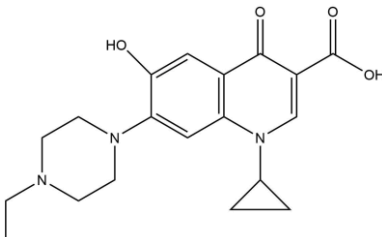
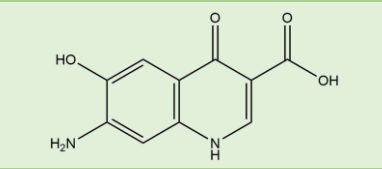
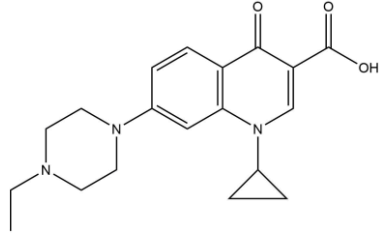
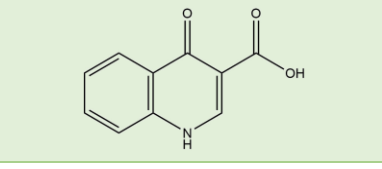
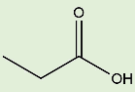
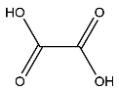
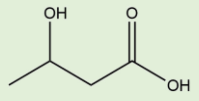
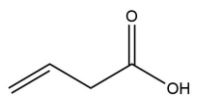
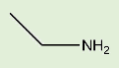


Fig. S7 DMPO spin-trapping ESR spectra for the Ag-ZnFe₂O₄-rGO in aqueous dispersion for (A) DMPO-•OH and methanol dispersion for (B) DMPO-•O₂⁻.

Table. S2 Degradation products of ENR by visible-light activated Ag-ZnFe₂O₄-rGO.

Products	Fragment Information (m/Z)	Retention Time (t _R)/min	Collision Energy /V	Molecular Formula	Supposed Structure
P1	341	39	20	C ₁₉ H ₂₃ N ₃ O ₃	
P2	357	44	20	C ₁₉ H ₁₃ N ₃ O ₄	
P3	220	28	20	C ₁₃ H ₁₇ N ₂ O ₄	
P4	189	11	20	C ₁₀ H ₇ NO ₃	
P5	191	8	20	C ₁₀ H ₉ NO ₃	
P6	42	6.5	20	CH ₂ N ₂	<chem>HN=C=NH</chem>
P7	74	6.7	20	C ₃ H ₆ O ₂	
P8	90	7.1	20	C ₂ H ₂ O ₄	
P9	104	7.5	20	C ₄ H ₈ O ₃	
P10	86	7.7	20	C ₄ H ₆ O ₂	
P11	45	6.4	20	C ₂ H ₇ N	

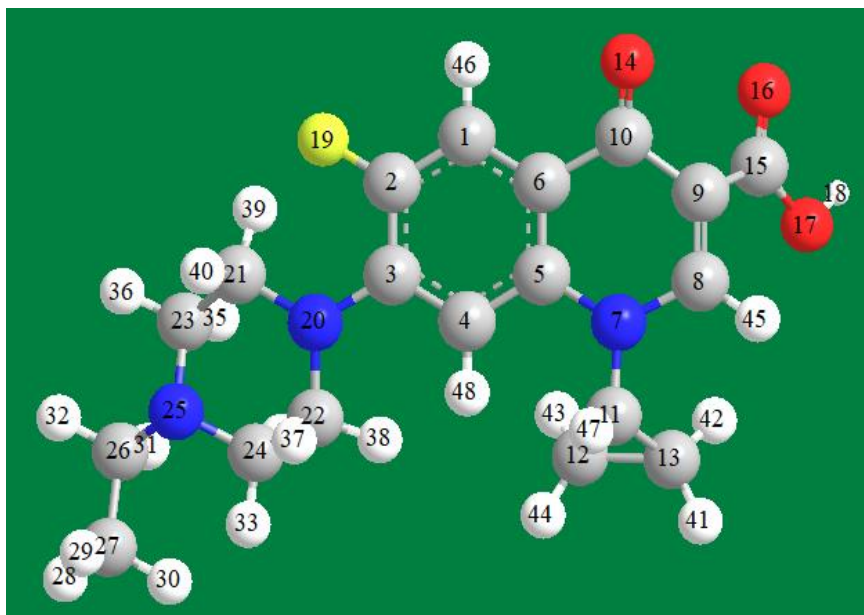


Fig. S8 The optimized conformation of ENR.

References

- (1) Guo, H.; Jiang, N.; Wang, H.; Lu, N.; Shang, K.; Li, J.; Wu, Y. Pulsed discharge plasma assisted with graphene–WO₃ nanocomposites for synergistic degradation of antibiotic enrofloxacin in water. *Chem. Eng. J.*, **2019**, 372, 226–240.
- (2) Xue, W.; Huang, D.; Li, J.; Zeng, G.; Deng, R.; Yang, Y.; Chen, S.; Li, Z.; Gong, X.; Li, B. Assembly of AgI nanoparticles and ultrathin g-C₃N₄ nanosheets codecorated Bi₂WO₆ direct dual Z-scheme photocatalyst: An efficient, sustainable and heterogeneous catalyst with enhanced photocatalytic performance. *Chem. Eng. J.*, **2019**, 373, 1144–1157.
- (3) Yan, W.; Yan, L.; Jing, C. Impact of doped metals on urea-derived g-C₃N₄ for photocatalytic degradation of antibiotics: Structure, photoactivity and degradation mechanisms. *Appl. Catal. B Environ.*, **2019**, 244, 475–485.
- (4) Huang, P.; Luan, J. Dispersed GaOOH rods loaded on the surface of ZnBiNbO₅ particles with enhanced photocatalytic activity toward enrofloxacin. *RSC Adv.*, **2019**, 9, 32027.